



## Relation between Silver Surface Roughness and Optical Properties: Scanning Tunneling Microscopy, Photoemission and Raman Scattering Continuum

Giovanni Aloisi,<sup>a</sup> Maurizio Muniz-Miranda,<sup>a</sup> Rolando Guidelli,<sup>a</sup> Alexander M. Funtikov<sup>b</sup> and Vladimir E. Kazarinov,<sup>a,b</sup>

<sup>a</sup> Dipartimento di Chimica, Università di Firenze, 50121 Firenze, Italy. Fax: +39 55 354 845

<sup>b</sup> A. N. Frumkin Institute of Electrochemistry, Russian Academy of Sciences, 117071 Moscow, Russian Federation. Fax: +7 095 952 0846

A silver (111) single crystal electrode was roughened in perchlorate solution by a non-conventional oxidation–reduction cycle. The topography of the roughened electrode surface, as determined by *in situ* STM, was correlated with two optical properties, namely, local photoemission and Raman scattering continuum. An enhancement of these optical properties due to atomic-scale surface features was found and the relationship between this enhancement and the photoexcitation of electron-hole pairs on the electrode surface is discussed.

It is well known that Raman scattering (RS) continuum and photoemission currents are strongly enhanced on rough metal surfaces, just as RS of adsorbed molecules.<sup>1–8</sup>

Surface enhanced Raman scattering (SERS) is often interpreted in terms of the creation of electron-hole (e–h) pairs at the surface by incident photons: inelastic scattering of electrons by adsorbate vibrations before the recombination of e–h pairs is regarded as being responsible for photon emission at a frequency shifted with respect to that of the incident light,<sup>1,6,7</sup> while the excitation of e–h pairs near the metal surface is accompanied by emission of part of the electrons into the electrolyte solution, namely by external photoemission,<sup>9,10</sup> as well as by annihilation of e–h pairs with a continuous energy spectrum resulting in the RS continuum.<sup>1,6,11</sup> Surface plasmons are assumed to enhance both excitation and annihilation of e–h pairs<sup>6</sup> and this conventionally explains the strong enhancement of both the RS continuum and RS of adsorbed molecules on a silver surface roughened by an oxidation reduction cycle (ORC)

The potential of *in situ* scanning tunneling microscopy (STM)<sup>12</sup> in providing the topography of an electrode surface<sup>13</sup>

can be conveniently exploited to correlate the surface morphology with the efficiency of e–h pairs generation. In this note an Ag(111) single crystal face was roughened by a particular ORC which was found to ensure a stable and reproducible optical response at far negative potentials.<sup>8,14</sup> The same surface and ORC roughening were used for both STM and optical measurements.

Water was obtained from light mineral water by distilling it once, and by then distilling the water so obtained from alkaline permanganate, while constantly discarding the heads. Merck KClO<sub>4</sub> was recrystallized from distilled water, and then dried. All measurements were carried out in aqueous 0.07 mol dm<sup>–3</sup> KClO<sub>4</sub> at room temperature, 23 ± 1 °C. All potentials are referred to the saturated calomel electrode (SCE). The experimental set up for STM measurements and the procedure adopted have been described elsewhere.<sup>15</sup>

The Ag(111) single crystal electrode was a cylinder 4 mm in diameter and 3 mm in height which had been grown by zone melting of 99.99% purity silver powder. Its orientation was known to ± 1.5°. The electrode was polished mechanically with

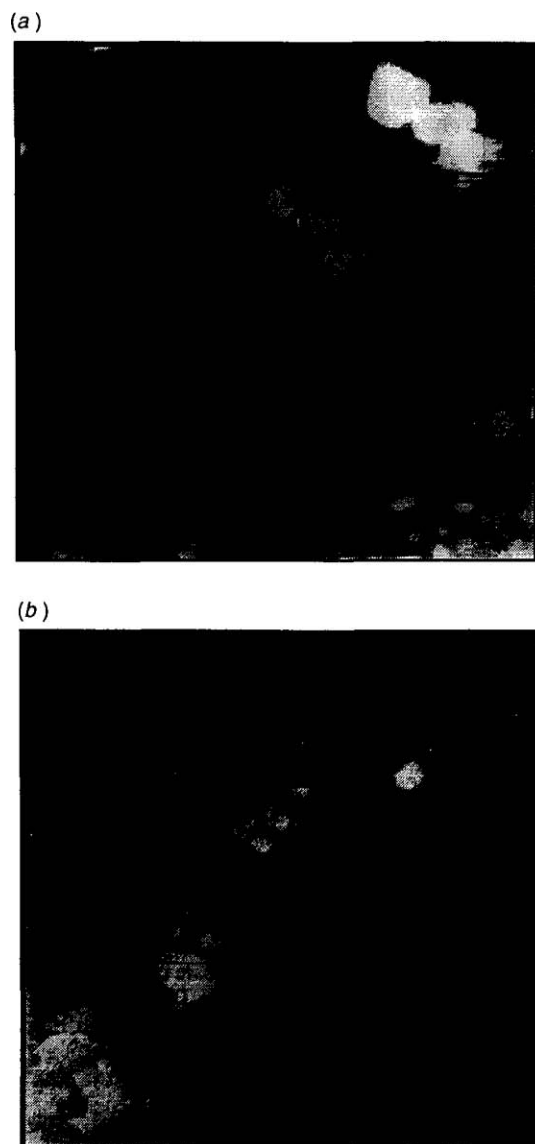


Fig. 1  $800 \times 800 \text{ \AA}$  STM images of an Ag(111) single crystal face after an ORC involving the dissolution and redeposition of 2 to 3 monolayers. Height excursion:  $20 \text{ \AA}$ . Electrode potential:  $-1.3 \text{ V}$  (a) and  $-0.5 \text{ V}$  (b).

$1 \mu\text{m}$  alumina and was then repeatedly treated with  $\text{CrO}_3$ <sup>16</sup> until a smooth, mirror-like surface was obtained. Before measurements the surface was etched with a 1:1 mixture of 40% hydrogen peroxide and 30% ammonia for a few seconds. Subsequently it was roughened in aqueous  $0.07 \text{ mol dm}^{-3}$   $\text{KClO}_4$  by sweeping the applied potential in the positive direction at a sweep rate of  $20 \text{ mV s}^{-1}$  until the desired quantity of silver was dissolved and by then sweeping it back, at  $5 \text{ V s}^{-1}$  to the final value of  $-1.3 \text{ V/SCE}$  to cause  $\text{Ag}^+$  deposition.<sup>8</sup>

The cell for optical measurements was made of glass. The counter electrode consisted of a gold coil, whereas the reference electrode consisted of an external molar calomel electrode (MCE). The hanging solution method<sup>17</sup> was employed to make contact between the silver crystal face and the solution. The three electrodes were connected to a PG28 Heka potentiostat, which also allowed the measurement of the charge involved in silver dissolution during the positive potential sweep of the ORC. Both a  $\text{Kr}^+$  100 mW laser (407 and 647 nm lines) and a  $\text{Ar}^+$  100 mW laser (488 nm lines) were used. The laser beam was reflected by a mirror on a spot of the electrode surface through the optically flat bottom of the cell with an angle of incidence of  $60^\circ$ . The electrode surface was parallel to the bottom of the cell, at a distance of about  $0.5 \text{ cm}$  from it, and the scattered light was collected in the direction normal to the electrode surface and

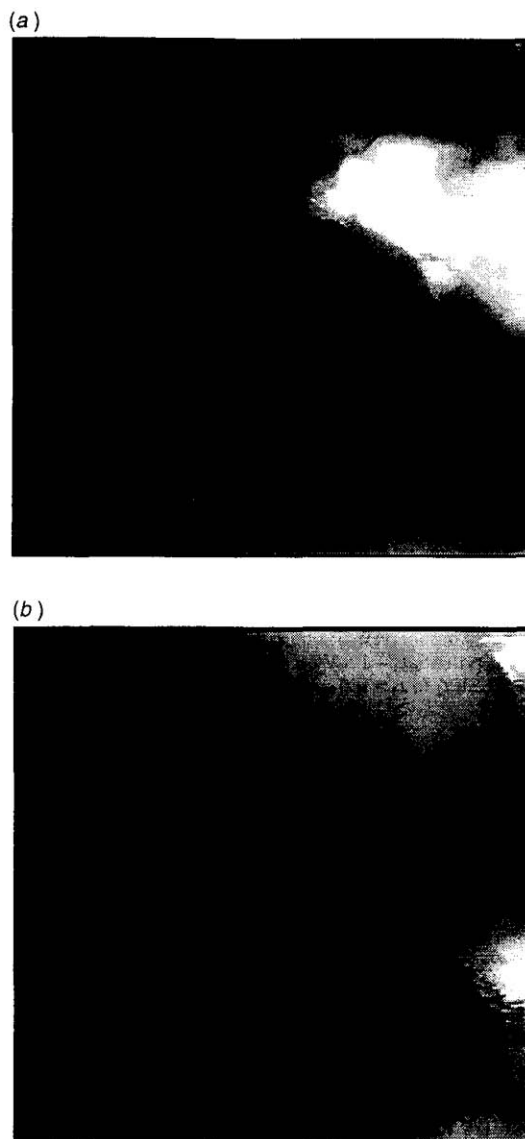


Fig. 2  $1520 \times 1520 \text{ \AA}$  STM images of an Ag(111) single crystal face after an ORC involving the dissolution and redeposition of *ca.* 30 monolayers. Height excursion:  $500 \text{ \AA}$ . Electrode potential:  $-1.3 \text{ V}$  (a) and  $-0.2 \text{ V}$  (b).

reflected on the slit of a scanning spectrometer system based on a Jobin-Yvon HG2S monochromator, a cooled RCA-C31034A photomultiplier, a photon counting system and a data acquisition facility.

The RS continuum was measured at a Raman shift  $\Delta\nu = 900 \text{ cm}^{-1}$ . Photoemission measurements were carried out in parallel with RS continuum measurements by chopping the laser beam at a frequency of 35 Hz and by measuring the in-phase current with a 128A PAR lock-in amplifier. Photoemission currents were measured in the absence of scavengers and were therefore produced by the bimolecular reaction of solvated electrons.<sup>8,14</sup> Focusing the laser beam on a spot of the electrode surface with a diameter of *ca.*  $200 \mu\text{m}$  permitted a comparatively high counting rate of the RS continuum and a sufficiently high efficiency of the bimolecular reaction of solvated electrons.

Fig. 1(a) shows the STM image of the electrode surface at  $-1.3 \text{ V}$  just after an ORC involving the dissolution and subsequent redeposition of 2 to 3 silver monolayers.<sup>15</sup> The surface is covered with bumps 30 to  $100 \text{ \AA}$  in diameter and  $4$  to  $20 \text{ \AA}$  in height. On stepping the potential to  $-0.5 \text{ V}$  [see Fig. 1(b)] most of these bumps disappear. Fig. 2(a) shows the electrode surface after an ORC involving the dissolution and redeposition of *ca.* 30 silver monolayers. We now observe much larger bumps,  $100$  to  $200 \text{ \AA}$  in diameter and  $10$  to  $60 \text{ \AA}$  in height. Smaller

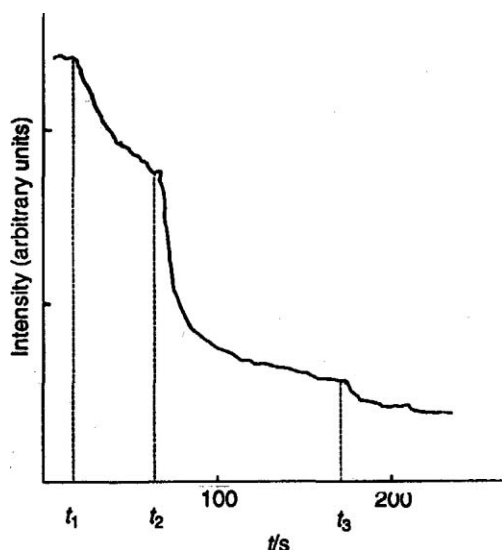


Fig. 3 Time dependence of the RS continuum intensity at an Ag(111) single crystal face in aqueous  $0.07 \text{ mol dm}^{-3} \text{ KClO}_4$  after an ORC involving 30 monolayers. Raman shift:  $900 \text{ cm}^{-1}$ . Exciting line  $407 \text{ nm}$ . Electrode potential:  $-1.5 \text{ V}$  up to  $t_1 = 10 \text{ s}$ ,  $-1.3 \text{ V}$  from  $t_1$  to  $t_2 = 60 \text{ s}$ ,  $-0.5 \text{ V}$  from  $t_2$  to  $t_3 = 160 \text{ s}$ ,  $-0.2 \text{ V}$  from  $t_3$  onward.

bumps, if present, are not visible because the vertical scale of the STM image is too large to allow the resolution of features a few Ångströms high. Upon shifting the applied potential to  $-0.5 \text{ V}$  these bumps are left unchanged, although a further shift to  $-0.2 \text{ V}$  causes them to disappear, as shown in Fig. 2(b).

The ORC adopted in Fig. 1 proved inadequate to produce a detectable surface enhancement. Hence the ORC used in Fig. 2, corresponding to the dissolution and redeposition of *ca.* 30 silver monolayers, was constantly adopted in the optical measurements. The RS continuum measured on this surface exhibited an almost constant intensity for shifts ranging from  $400$  to  $2000 \text{ cm}^{-1}$ ; a  $900 \text{ cm}^{-1}$  Raman shift was chosen for our measurements. After the ORC an RS continuum intensity nearly constant in time was obtained only at a redeposition potential as negative as  $-1.5 \text{ V}$ . Incidentally, this is the most negative potential which can be applied to the silver electrode in perchlorate solution without appreciable hydrogen evolution. When less negative redeposition potentials were adopted the RS continuum intensity attained a maximum after *ca.* 1 min from the ORC and then decreased progressively. The effect of stepping the potential from  $-1.5 \text{ V}$  towards less negative values is shown in Fig. 3. Stepping the potential to  $-1.3 \text{ V}$  at time  $t_1 = 10 \text{ s}$  caused a decrease of *ca.* 20–30% in the RS continuum intensity during the time interval from  $t_1$  to  $t_2 = 60 \text{ s}$ . A further potential step to a substantially less negative potential,  $-0.5 \text{ V}$ , at time  $t_2$  caused a much more rapid decay in the RS continuum intensity. A further moderate decrease was observed upon stepping the potential to  $-0.2 \text{ V}$  at  $t_3 = 160 \text{ s}$ . Nearly the same transients were observed using  $488$  and  $647 \text{ nm}$  excitation lines; with the latter excitation line the counting rate was about one order of magnitude lower than with the  $407 \text{ nm}$  line. In all cases the changes in photocurrent ran in parallel with those in the RS continuum intensity.

A more quantitative estimate of the effect of the electrode potential on the RS continuum intensity as well as on the photocurrent was obtained by the following procedure. The instantaneous condition of the electrode surface at any applied potential, with regard to both RS continuum intensity and photocurrent, can be 'frozen' indefinitely by stepping the potential to  $-1.5 \text{ V}$ . The electrode was then normally kept at  $-1.5 \text{ V}$  and the potential was stepped to different, progressively more positive potentials, held at these potentials for  $100 \text{ s}$  and then stepped back to  $-1.5 \text{ V}$  where the RS continuum intensity and the photocurrent were measured.

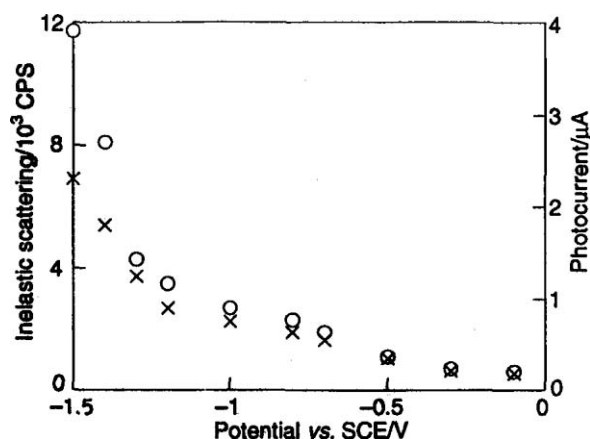
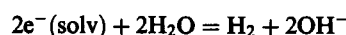


Fig. 4 Plots of the RS continuum intensity (○) and of the photocurrent (×) against potential at an Ag(111) single crystal face in aqueous  $0.07 \text{ mol dm}^{-3} \text{ KClO}_4$  solution after an ORC involving 30 monolayers (see the text for details). Raman shift:  $900 \text{ cm}^{-1}$ .

The results are summarized in Fig. 4. Both RS continuum intensity and photocurrent decrease as the exposure potential becomes progressively more positive. At first sight it seems puzzling that such a decrease, which amounts to about one order of magnitude for a potential step from  $-1.5$  to  $-0.5 \text{ V}$ , does not correspond to any apparent change in surface topography when passing from Fig. 2(a) to Fig. 2(b). This apparent contradiction can be resolved if we make the reasonable assumption that the changes in the small-scale structural defects as observed on a much less roughened electrode surface in passing from Fig. 1(a) to Fig. 1(b), are also present under the experimental conditions of Fig. 2, where they cannot be detected due to insufficient instrumental resolution. In fact the STM feedback parameters, tuned to follow the profiles of large-scale structural defects, do not permit us to single out the small-scale ones, if present. Now, the atomic-scale structural defects in Fig. 1(a) could hardly change the conditions for the excitation of both delocalized surface plasmons<sup>18</sup> and local dipolar plasma resonances or local modes.<sup>19,20</sup> We are therefore led to ascribe the appreciable influence of these atomic-scale surface structures on the efficiency of e-h pair excitations to an increase in the matrix elements of intraband optical transitions near the surface<sup>7,8</sup> rather than to changes in the local electromagnetic field. Several causes of enhancement of photon-electron coupling due to atomic-scale roughness or surface disordering are described in ref. 7.

At any rate, the overall enhancement of local photoemission currents is mainly determined by the excitation of local modes. In this connection it must be stressed that in our experiment photoemission currents were measured in the absence of scavengers added on purpose, and hence the capture of solvated electrons in solution was mainly determined by the reaction:<sup>14</sup>



which is of second order with respect to the solvated electrons. This implies an enhancement of the local electromagnetic field intensity by at least four or five orders of magnitude near structural features with appropriate geometry for local mode excitation such as those in Fig. 2(a). These features are stable at  $-0.5 \text{ V}$  and hence, even upon exposure of the silver electrode to  $-0.5 \text{ V}$ , the enhancement is high enough to provide measurable photocurrents. It should be stressed that the above conclusions modify the point of view<sup>8,14</sup> according to which the whole photocurrent enhancement is due to a local field enhancement resulting from the excitation of local modes. Exposure of the silver electrode to a potential as positive as  $-0.2 \text{ V}$ , as done in Fig. 3, leads to the loss of the non-linear dependence of the measured photocurrent on light power; under these conditions the residual photocurrent is to be ascribed to scavenger

impurities present in the solution. The STM image in Fig. 2(b), obtained under the same experimental conditions, exhibits a surface topography in which the root mean squared heights are much less than the correlation length. Hence this surface topography is more suitable for the excitation of delocalized surface plasmons than for the excitation of local modes. Over this potential range it is difficult to separate the contributions to the RS continuum from local modes and from delocalized surface plasmons due to the additional contribution from the normal RS of water.

Thanks are due to the Italian Consiglio Nazionale delle Ricerche (CNR) for financial support. This work is part of a joint project between the Russian Academy of Sciences and the Progetto Finalizzato Chimica Fine II of the Italian CNR.

## References

- 1 *Surface Enhanced Raman Scattering*, eds. R. K. Chang and T. Furtak, Plenum, New York, 1982.
- 2 A. Otto, in *Light Scattering in Solids*, eds. M. Cardona and Guntherodt, Springer, Berlin, 1984, vol. IV, ch. 6.
- 3 M. Moskovits, *Rev. Mod. Phys.*, 1985, **57**, 296.
- 4 R. L. Birke and J. R. Lombardi, in *Spectroelectrochemistry*, ed. R. J. Gale, Plenum, New York, 1988.
- 5 B. Pettinger, in *Adsorption of Molecules at Metal Electrodes*, VCH, New York, 1992, p. 285.
- 6 E. Burstein, Y. J. Chen, C. Y. Chen, S. Lundquist and E. Tosatti, *Solid State Comm.*, 1978, **29**, 567.
- 7 A. Otto, T. Bomemann, U. Ertürk, I. Mrozek and C. Pettenkofer, *Surface Sci.*, 1989, **210**, 363.
- 8 A. M. Funtikov, S. K. Sigalaev and V. E. Kazarinov, *J. Electroanal. Chem.*, 1987, **228**, 197.
- 9 G. C. Barker, *Electrochim. Acta*, 1968, **13**, 1221.
- 10 A. M. Brodsky and Yu. Ya. Gurevich, *Zh. Eksp. Teor. Fiz.*, 1968, **27**, 114 (in Russian).
- 11 R. L. Birke, J. Lombardi and J. I. Gersten, *Phys. Rev. Lett.*, 1979, **43**, 71.
- 12 G. Binnig, H. Rohrer, Ch. Gerber and E. Weibel, *Phys. Rev. Lett.*, 1982, **49**, 57.
- 13 J. Wiechers, T. Twomey, D. M. Kolb and R. J. Behm, *J. Electroanal. Chem.*, 1988, **248**, 451.
- 14 A. M. Funtikov, S. K. Sigalaev and V. E. Kazarinov, *Electrokhimiya*, 1989, **25**, 762 [*Sov. Electrochem. (Engl. Transl.)*, 1989, **25**, 677].
- 15 G. Aloisi, A. M. Funtikov and R. Guidelli, *Surface Sci.*, in press.
- 16 A. Hamelin, L. Doubova, L. Stoicoviciu and S. Trasatti, *J. Electroanal. Chem.*, 1988, **244**, 133.
- 17 R. Guidelli, M. L. Foresti, A. M. Funtikov and M. Muniz-Miranda, *J. Electroanal. Chem.*, 1993, in press.
- 18 H. Raether, in *Surface Polaritons*, eds. V. M. Agranovich and D. L. Mills, North Holland, Amsterdam, 1982, p. 331.
- 19 J. I. Gersten and A. Nitzan, *J. Chem. Phys.*, 1980, **73**, 3023.
- 20 M. Kerker, D. S. Wang and H. Chew, *Appl. Opt.*, 1980, **19**, 415.

Received: Moscow, 29th June 1993

Cambridge, 27th August 1993; Com. 3/04002J